Emission decay and energy transfer in Yb/Tm Y-codoped fibers based on nano-modified glass

Dmitry Klimentov[a,*], Vladislav V. Dvoyrin[a], Arindam Halder[b], Mukul Chandra Paul[b], Shyamal Das[b], Mrinmay Pal[b], Shyamal K. Bhadra[b], and Irina T. Sorokina[a]

[a] *Department of Physics, Norwegian University of Science and Technology, N-7491 Trondheim, Norway,* dmitry.klimentov@ntnu.no, +4793452830
[b] *Fiber Optics and Photonics Division CSIR-Central Glass & Ceramic Research Institute, 196, Raja S.C.Mullick Road, Jadavpur, Kolkata-32, India*

Abstract: We report the results of experimental investigation and theoretical analysis of luminescence decay in Yb/Tm Y-codoped fibers based on nano-modified glass. Based on the experimental results, numerical simulations allowed us to estimate the energy transfer efficiency between Yb^{3+} and Tm^{3+} ions. It was shown that yttria enhances the Yb/Tm energy transfer making fibers with Y-codoping promising for development of the light sources for laser applications and of up-conversion emitters for visualization applications. These fibers demonstrate energy transfer efficiency of ~50 %, which makes them attractive for diode-pumping of Yb-ions at 975 nm wavelength.

Keywords: Fiber optics, Infrared fiber lasers, Energy transfer

1. Introduction

The interest to Yb/Tm-doped fibers and crystals is caused by the possibility of their direct pumping by conventional low cost telecom diode lasers operating at 975 nm [1-3] - an alternative pumping method of Tm, when simple and cost-effective low- to medium power Tm-fiber sources are sought. In this context the investigation of efficiency of the energy transfer (ET) from Yb^{3+} to Tm^{3+} ions becomes of great importance [4,5]. This efficiency is known to be dependent on the fiber composition. The spectroscopic investigation of Yb/Tm-doped fibers codoped with yttria was reported recently in [6]. It was assumed that yttria allows enhancing the Yb-Tm ET. The subject of this work is the investigation of the ET processes between Yb^{3+} and Tm^{3+} ions in relation to the new compositions of core glass of Yb/Tm-doped Y-codoped fibers.

For Yb/Tm system the efficiency of the ET from Yb^{3+} to Tm^{3+} ions reaches 50% [7]. The typical lifetimes for the $^3F_4$ level of Tm^{3+} vary from 200 to 650 μs, and for the $^2F_{5/2}$ level of Yb^{3+} from 470 to 830 μs depending on the host composition [4, 8-10]. Despite the large importance of the ET processes, there are not so much data in the literature on the efficiency of the ET from Yb^{3+} to Tm^{3+} ions, which makes our work particularly relevant.

In this paper we report the results of the measurements of Yb^{3+} luminescence decay in the presence of Tm^{3+} ions in Y-codoped silica glass fibers based on nano-modified glass, the decay time of Tm^{3+} ions as well as the calculations of the ET efficiency in the set of Yb/Tm-doped fibers with different doping concentration levels. The technological processes as well as the effect of nano-engineering of the glass host and its influence on the ET efficiency are also being discussed in this paper. The purpose of such nano-engineering is to increase the ET efficiency from Yb^{3+} to Tm^{3+} ions thus making such fibers promising for development of the light sources for laser applications and of the up-conversion emitters for visualization applications [11].

2. Fiber fabrication and material analysis

In our experiment we have studied the set of Yb/Tm-doped silicate fibers, namely: LCT-6, LCT-8 [6], and newly produced LCT-9, LCT-10, and HTY-1 fibers with different concentrations of dopants. The waveguide parameters of the fibers are presented in Table 1, the compositions as well as the calculation and measurement results are given in Table 2. Typical luminescence and optical absorption spectra are presented in Fig.1.

Table 1. Waveguide parameters of the fibers under investigation

Fiber Sample	Core diameter, μm	Numerical Aperture
LCT-9	18.0	0.29
LCT-6	15.8	0.22
LCT-10	10.0	0.23
LCT-8	14.2	0.26
HTY-1	8.0	0.16

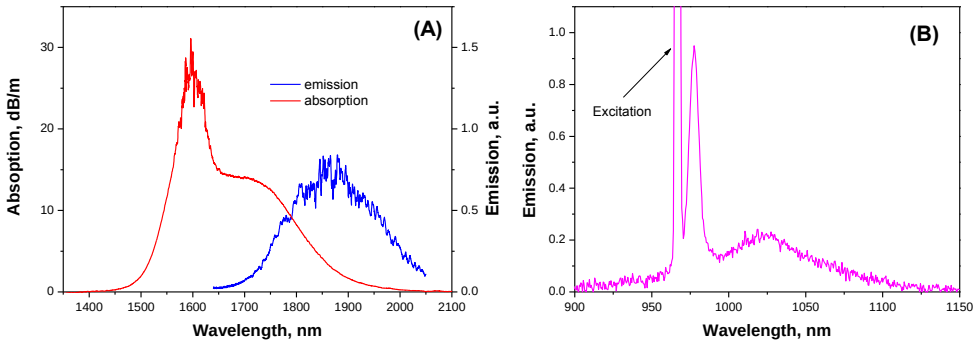

Fig. 1. Typical absorption and emission spectra of Tm^{3+} (A), and emission spectrum of Yb^{3+} (B).

Yb/Tm co-doped yttrium-alumino-silicate (YAS) fibers were fabricated by modified chemical vapor deposition (MCVD) process in conjunction with solution doping (SD) technique. Since 1987, SD technique has been used to incorporate rare-earths [12] and nano-particles [10, 13-16] into the silica glass matrix of optical fibers.

We assume that Y-codoping allows modification of the fiber glass by creation of the nano-structures with high active ion concentration. We have studied the nature of the nano-structures in the core glass of our samples by the transmission electron microscopy (TEM). The TEM image of the core region of the LCT-9 fiber is shown in Fig. 2(A). This image suggests that the two separate phases are formed inside the core. The granules of the diameter around 0.5 - 5 nm with dark appearance are formed mainly by the atoms with high atomic mass. The glass outside the black granules is formed mainly by the atoms with lower atomic mass. For the proper analysis of the nature of these phases the Electron Diffraction (ED) pattern (Fig. 2(B)) and EDX analysis were performed. The diffraction pattern showed that the black particle-like granular features have amorphous nature. EDX spectra taken ‘on’ and ‘outside’ the granules shown in Fig. 2(C) and Fig. 2(D) showed that the black granules are formed by Y, Al, Tm, Yb and Si oxides. The other part of the matrix outside the dark granules is constructed mostly by the Si-oxide with a trace of Al. It was found from EDX that Tm and Yb are concentrated mainly within the black granules.

From this analysis we can say that the black phases correspond to YAS glass phases and form the hosts for active Tm^{3+} and Yb^{3+} ions in the core. From the TEM images it is also seen that the YAS glass phases are distributed almost homogeneously in the silicate glass in the form of nano-phases. Thus, these YAS phases help Tm and Yb to be distributed homogeneously in the core. This analysis also cleared that there is a rear-earth-rich (RE-rich) and RE-poor zones within the core. Particularly, the nano YAS phases are the RE-rich zones.

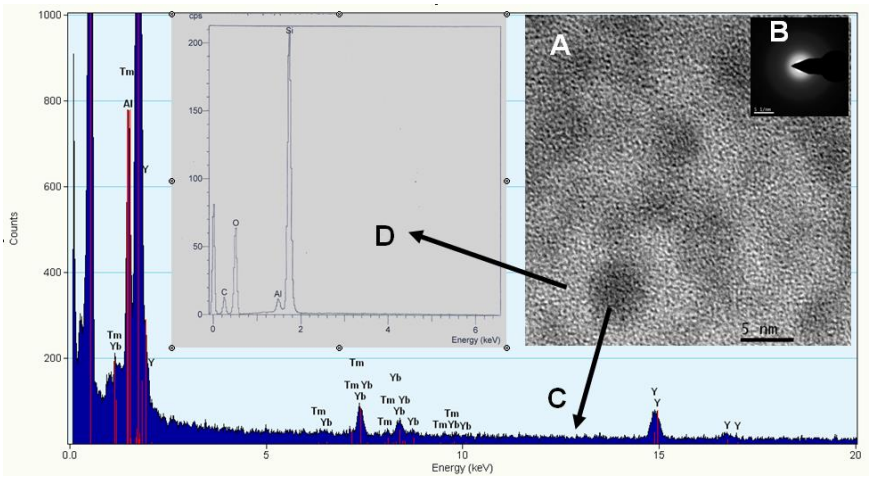

Fig. 2. (A) TEM image and (B) electron diffraction pattern of the fiber (LCT-9),
(C) EDX plot taken on and (D) outside of black spots of the fiber sample.

Typical microscopic view of the fiber LCT-9 sample is shown in Fig. 3(A). The refractive index profile of the fiber preform LCT-8 sample measured by the preform analyzer is shown in Fig. 3(B). The dopants' concentrations along the core diameter were measured by the electron probe micro-analysis (EPMA). The dopants' distribution of the fiber LCT-10 sample is shown in Fig. 3(C), and for the other samples it is given in Table 2.

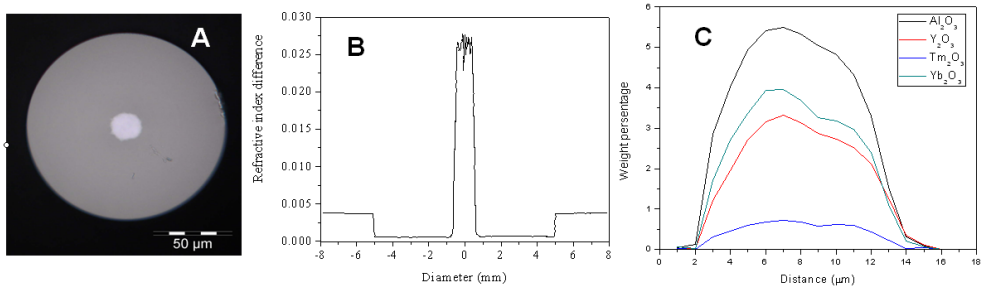

Fig. 3. (A) The microscopic cross-sectional view of the fiber sample (LCT-9),
(B) Refractive index profile of fiber perform sample (LCT-8) and
(C) EPMA curve for distribution of different dopants along the diameter of fiber sample (LCT-10).

Due to the small size (0.5 – 5.0 nm) of nano YAS-RE phases, fibers exhibit negligible Rayleigh scattering losses [16]. To estimate the possible scattering losses caused by the nano-phases we have performed the loss measurements of the fiber samples. The spectral loss curve of the LCT-8 fiber is shown in Fig. 4. The absorption spectrum of the fiber sample was measured at the wavelength range of 350 – 1700 nm. The absorption peak of Yb^{3+} obtained at 975 nm can be associated with a hump at 920 nm due to the transitions from $^2F_{7/2}$ to $^2F_{5/2}$ levels. In case of Tm^{3+} ions, there are three electronic transitions involved: $^3H_6 \rightarrow {}^3H_4$, $^3H_6 \rightarrow {}^3F_{2,3}$, $^3H_6 \rightarrow {}^1G_4$, which correspond to the absorption peaks at 789 nm, 678 nm and 465 nm respectively [17-18]. Another absorption peak of Tm^{3+} is also observed at 1205 nm in the attenuation spectra, which represents the electronic transition from $^3H_6$ to $^3H_5$ level.

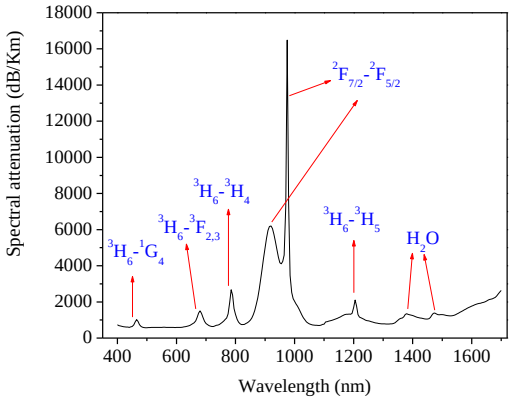

Fig. 4: Spectral attenuation curve of the Tm/Yb codoped fiber (LCT-8).

3. Experimental

To find the efficiency of the ET between Yb^{3+} and Tm^{3+} ions and the dopants' effective lifetimes, we examined luminescence decay kinetics of Yb^{3+} $^2F_{5/2}$ and Tm^{3+} $^3F_4$ levels after pulsed excitation by two diode lasers: one with the emission wavelength of 980 nm for the ET efficiency measurement and the other with the wavelength of 1550 nm for the effective lifetime measurements of Tm^{3+} ions.

Three photodetectors were used for the kinetics detection: Ge photodetector operating in 0.8 – 1.8 μm range (ThorLabs PDA50B-EC), Si photodetector (0.4 – 1.1 μm) (ThorLabs FDS1010) and extended InGaAs photodetector (1.2 – 2.55 μm) (Hamamatsu G5853-23). Ge and Si photodetectors allowed measuring the kinetics of Yb^{3+} ions. Due to fast drop of its sensitivity at the longer wavelength edge the possible impact of Tm emission was negligible. On the other hand, InGaAs photodetector allowed us measuring the kinetics of $^3F_4$ level of Tm^{3+} ions. That choice of the detectors ensured the spectral separation of our measurements.

Both sources were supplied with electrical pulses of 1 ms duration, at the frequency of 89 Hz, with fall-of time of 1 μs. The optical pulses with average excitation power of around 10 mW were produced. The fall-off times measured with Ge and Si detectors were 15 μs and the fall-off time measured with InGaAs detector was 40 μs, respectively. This elongation is mainly attributed to the detectors' response. The decays were detected from the outer fiber surface and recorded with a digital Instek GDS-3354 oscilloscope.

3. Results

The decays of $^3F_4$ level of Tm^{3+} ions obtained under 1550 nm excitation and collected by InGaAs were exponential, while the decays of Yb^{3+} ions obtained under 980 nm excitation were non-exponential. The kinetics for the fibers (LCT-9 and LCT-6) are shown in Fig. 5. and Fig. 6.

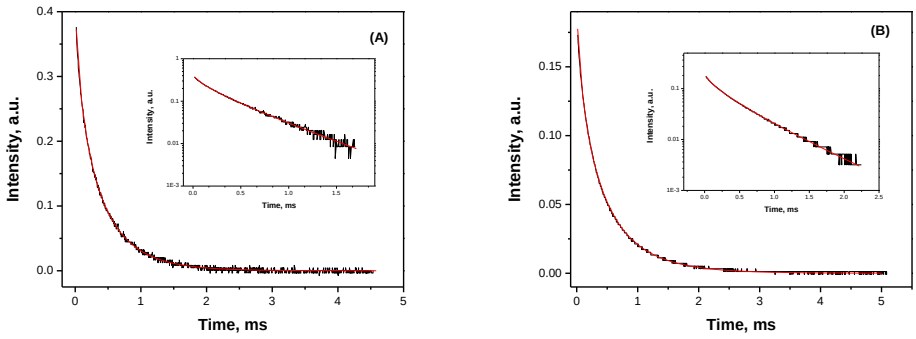

Fig. 5. Typical non-exponential decays with excitation at 980 nm wavelength corresponding to the energy transfer between the ions, measured with Ge photodetector, the black line corresponds to the experimental data and the red one is the approximated using the eq.(2). The inset is in logarithmic scale. (A) LCT-9 and (B) LCT-6 fibers.

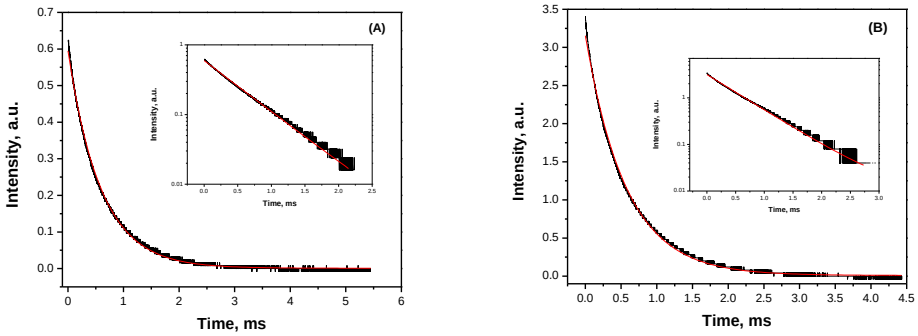

Fig. 6. Tm^{3+} kinetics with the excitation wavelength of 1550 nm, measured by InGaAs photodetector, the black line corresponds to the experimental data and the red one is the exponential fitting of the curve. The inset is in logarithmic scale. (A) LCT-9 and (B) LCT-6 fibers.

Since the decay kinetics of the Yb^{3+} ions were not exponential, the effective decay constant τ_{eff}, of Yb kinetics was calculated using eq.(1). These kinetics were also approximated using the eq.(2) (Inokuti-Hirayama formula [19]), which describes the donor fluorescence kinetics under the assumption of dipole-dipole interaction between donor and acceptor for migration-assisted ET [20]. The migration-assisted and direct donor–acceptor energy-transfer rates were also obtained from the fitting of the kinetics using eq.(2). The ET-efficiency η was calculated using the eq.(3) [21] and reached 56% for LCT-9 fiber, which is slightly higher than it was previously reported. For the calculations we used the value of Yb^{3+} lifetime (τ_{Yb}) equal to 830 μs that was measured for the Tm^{3+}-free fibers [4]. The comparable value of 810 μs of Yb^{3+} lifetime for Tm^{3+}-free fibers produced by the same technology with similar concentration was obtained in [10].

$$\tau_{eff} = \frac{\int I(t)tdt}{\int I(t)dt} \qquad (1),$$

$$I(t) = A_0 \exp\left(-\frac{t}{\tau_{Yb}} - \gamma t^{1/2} - Kt\right) \qquad (2),$$

$$\eta = 1 - \frac{\int I(t)dt}{A_0 \tau_{Yb}} \qquad (3),$$

where $I(t)$ is a decay kinetic, A_0 is the amplitude of the decay, K is the migration-assisted energy-transfer rate, and γ is the direct donor–acceptor ET rate.

The analysis of Tm^{3+} kinetics allowed us to determine the lifetime of $^3F_4$ level for all samples (Table 2). These values are comparable to the previously reported lifetimes (200-650 μs depending on the host [4, 8, 9]). During the fitting procedures the reduced chi-squared distribution of the fitting varied from 6.5×10^{-8} to 5.5×10^{-7} depending on the fiber, and the coefficient of determination (R^2) for all the samples was around 0.995. We estimated the standard deviation error in ET-efficiency to be around 2%.

Table 2. Summary of the parameters obtained in this work.

Sample	τ_{eff}, μs	τ_{Tm}, μs	Yb_2O_3, wt%	Y_2O_3, wt%	Al_2O_3, wt%	Tm_2O_3, wt%	γ	K, s^{-1}	η, %
LCT-9	450	590	4.5	4.0	6.0	1	39	226	56
LCT-6	520	570	2	1.9	2.0	0.8	33	105	49
LCT-10	540	510	4	3.3	5.5	0.7	22	547	46
LCT-8	570	570	2	3.0	1.0	0.5	23	279	42
HTY-1	720	400	0.9	2.5	4.5	0.75	20	466	21

The luminescence measurements of Tm-free Yb-doped fibers of similar composition produced with the same technology with the concentration of about 1.6 wt.% of Yb [10] showed that Yb^{3+} experiences single-exponential decay with a lifetime of about 800 μs. This value significantly exceeded the Yb decay constant τ_{eff} of the fibers with a similar concentration, LCT-6, LCT-8, see Table 2. Thus, the non-exponential decay with the lower constant as compared to the Yb lifetime in Tm-free samples is attributed to the ET between Yb^{3+} and Tm^{3+}, but not to the concentration quenching. We also conclude that the possible concentration quenching is not the critical issue for these fibers.

As it can be seen from Table 2, there is no influence of the Al concentration on the ET efficiency. But at the same time, one can see the direct proportionality between the Y concentration and ET efficiency. The double change in concentration of Y leads to the double change in the efficiency.

4. Discussion

The energy level diagram of the Tm/Yb system (Fig. 7. [4]) shows the processes of ET between the energy levels of Tm^{3+} and Yb^{3+} ions in the alumino-silicate host.

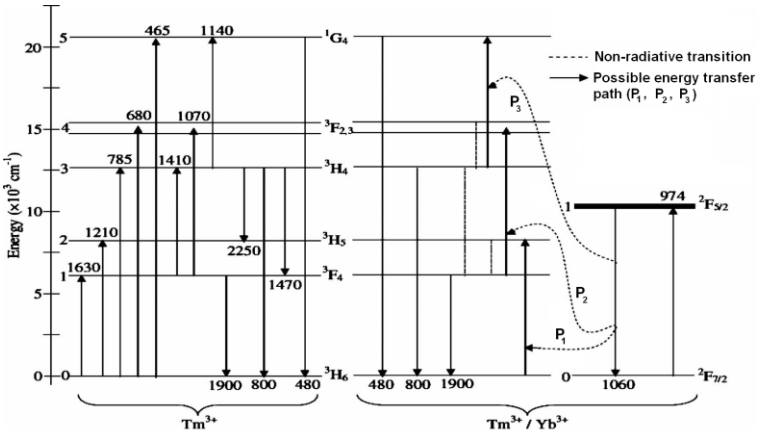

Fig. 7. Energy level diagram and energy-transfer processes in Tm3+/Yb3+ co-doped system [4].

According to the diagram, three transitions are possible in the Tm/Yb system: P_1, P_2 and P_3. The first transition results in the 2 μm emission and can be described as

$$Yb^{3+}(^2F_{5/2}) + Tm^{3+}(^3H_6) \rightarrow Yb^{3+}(^2F_{7/2}) + Tm^{3+}(^3H_5)$$

$$\rightarrow Yb^{3+}(^2F_{7/2}) + Tm^{3+}(^3F_4).$$

The P2 transition corresponds to the following relaxation/excitation scheme:

$$Yb^{3+}(^2F_{5/2}) + Tm^{3+}(^3F_4) \rightarrow Yb^{3+}(^2F_{7/2}) + Tm^{3+}(^3F_{2,3})$$

$$\rightarrow Yb^{3+}(^2F_{7/2}) + Tm^{3+}(^3H_4).$$

The third one results in population of the $^1G_4$ level, which is responsible for the 480 nm wavelength emission:

$$Yb^{3+}(^2F_{5/2}) + Tm^{3+}(^3H_4) \rightarrow Yb^{3+}(^2F_{7/2}) + Tm^{3+}(^1G_4).$$

We applied the commonly used Förster–Dexter [22] approach to the analysis of ET in Yb/Tm system, under the assumption of dipole-dipole interaction between donor and acceptor. As a consequence from this theory [19], the dependency of the direct donor–acceptor ET rate (γ) on the concentration of the acceptors (N_A) can be expressed by:

$$\gamma = \frac{4}{3}\pi^{\frac{3}{2}} N_A \sqrt{C_{DA}} \qquad (4)$$

where, C_{DA} is the donor-acceptor energy transfer microparameter and N_A is the concentration of the acceptors.

According to (4), there should be a linear dependence between γ and N_A. Such a linear behavior, Fig. 8(A). It means, that energy transfer processes in our Tm/Yb system can be described within the commonly applied Förster–Dexter theory under the assumption of dipole-dipole interaction.

At the same time, we have found that the efficiency of the ET linearly increases with the increase of the Thulium $^3F_4$ level lifetime, Fig. 8(B). To explain this phenomenon, we suggest the following mechanisms of the observed correlation. First, this dependence can be explained according to the diagram shown in Fig. 7. The increase of the $^3F_4$ level lifetime favors the up-conversion processes. Such processes terminating in $^1G_4$ energy level also increase the visible 480 nm wavelength emission intensity which can be interesting for certain applications [11].

Second, there is an obvious dependence of the ET-efficiency on the Y concentration that allows us to conclude that Y favors the energy transfer. Moreover, yttria allows enhancing the lifetime of Tm^{3+} in comparison to the Y-free silica hosts. We attribute it to the structural changes of the glass due to the addition of Y to the host. Indeed, the Y_2O_3 helps to create nano-structured YAS glass phase in the host and acts as a glass network generator [23-25]. The Al_2O_3 increases the refractive index (RI) of silica by $2.3x10^{-3}$ per mole and is used as intermediate core glass network modifier [26]. It helps to distribute Tm^{3+} and Yb^{3+} ions homogeneously to decrease phonon energy of silica glass [26]. The modified silica glass host is chosen due to its optical transparency from 200 nm to beyond 3000 nm wavelength region [27]. Furthermore, due to the lower phonon energy of YAS, the magnitude of radiative emission probability of metastable states of Tm^{3+} increases and the non-radiative multi-phonon decay decreases. This leads to the enhancement of the ET process from Yb^{3+} to Tm^{3+}ions. In this system the 975 nm excitation wavelength can be absorbed only by Yb^{3+}. Thus, the pump source excites the Yb^{3+} first and then the energy is transferred to nearby Tm^{3+} ion to excite it in an efficient manner.

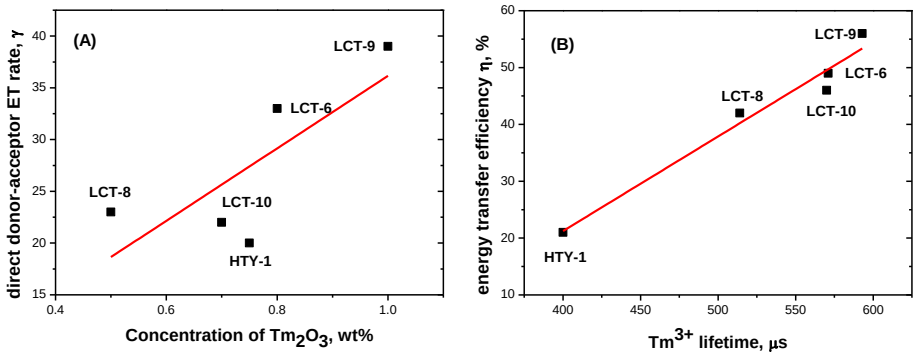

Fig. 8. (A) The dependency of direct donor-acceptor rate on the concentration of Tm_2O_3.
(B) Correlation between the transfer efficiency η and Tm^{3+} lifetime
(linear approximation by the straight line is shown as a guide-to the eye).

5. Conclusions

We measured the luminescence decay kinetics of the set of Yb/Tm nano-particles-doped silicate fibers codoped with yttria under excitation with the two pulsed diode lasers: one with the wavelength of 980 nm for the energy transfer analysis and the other with the wavelength of 1550 nm for the calculation of the Tm^{3+} $^3F_4$ level lifetime. We obtained from our experiment the average decay constants and the lifetimes of Tm^{3+} $^3F_4$ level, which varied from 490 to 890 μs and from 180 to 590 μs, respectively, depending on a fiber, as well as the energy transfer efficiency from Yb^{3+} to Tm^{3+} ions. The latter reached 56%. The correlation between the transfer efficiency and the $^3F_4$ level lifetime of Tm^{3+} was found and explained. The nano-engineering of the host by the Y_2O_3 doping allows to increase the efficiency of ET by creation of the nano-structures with the high doping levels of active Tm^{3+} and Yb^{3+} ions, which are organized in nano-phases. The Y_2O_3 effectively lowers the phonon energy and, as a consequence, increases the ET rates - the origin of the high up-conversion efficiency. The ET efficiency increases with the increase of the Y_2O_3 doping levels.

Up-conversion effects make these fibers attractive for development of cost-efficient up-conversion blue light emitters for visualization applications, as well as the effective energy transfer makes these fibers promising for development of Tm-doped fiber lasers pumped with the low-cost diodes operating at 975 nm wavelength.

Acknowledgements

The work has been supported by the NFR projects FRITEK/191614, MARTEC project MLR and EU-FET grant GRAPHENICS (618086), as well as by the Department of Science & Technology (DST), New Delhi, India.

References and links

[1] S. D. Jackson, "Power scaling method for 2 μm diode cladding-pumped Tm-doped silica fiber lasers that uses Yb codoping," Opt. Lett.**28**, (2003) 2192–2194.

[2] R.A. Hayward, W.A. Clarkson, P.W. Turner, J. Nilsson, A.B. Grudinin, D.C. Hanna, "Efficient cladding pumped Tm-doped silica fibre laser with high power single-mode output at 2 μm," Electron. Lett. **36**, (2000) 711-712.

[3] L. Batay, A. Demidovich, A. Kuzmin, A. Titov, M. Mond, S. Kuck, "Efficient tunable laser operation of diode-pumped Yb,Tm:KY(WO4)2 around 1.9 μm," Appl. Phys. B, **75**, (2002) 457-461.

[4] A. Pal, A. Dhar, S. Das, K. Annapurna, A. Schwuchow, T. Sun, K. Grattan, and R. Sen "Energy-transfer parameters in a Tm/Yb doped single mode silica fiber," J. Opt. Soc. Am. B. **27**, (2010) 2714-2720.

[5] D. Ghosh, H.T. Bookey, M.Pal, M.C. Paul, S.K. Bhadra and A.K. Kar, "Characterisation of Yb-Tm co-doped air-clad fibers for 2 μm laser applications," in proc. of 23rd Annual Meeting of the IEEE Photonics Society, (2010) 510-511.

[6] V. Dvoyrin, D. Klimentov, A. Halder, M. C. Paul, M. Palb, S. K. Bhadra, A. Kir'yanov, and I. Sorokina, "Novel Y2O3-codoped Yb/Tm-doped picosecond fiber laser," proc. SPIE **8601**, Fiber Lasers X: Technology, Systems, and Applications, 86012X, (2013).

[7] C. Jacinto, M. V. D. Vermelho, M. T. de Araujo, P. T. Udo, N. G. C. Astrath, A. C. Bento, T. Catunda, and M. L. Baesso "Thermal lens study of energy transfer in Yb3+/Tm3+-co-doped glasses,**"** Opt Exp, **15**, (2007) 9232-9238.

[8] P. Peterka, W. Blanc, B. Dussardier, G. Monnom, D. Simpson, and G. Baxter, "Estimation of energy transfer parameters in thulium-and ytterbium-doped silica fiber," Proc. SPIE **7138**, (2008) 71381K.

[9] S. D. Agger and J. H. Povlsen "Emission and absorption cross section of thulium doped silica fibers," Opt. Exp. **14**, (2006) 50-57.

[10] S. Yoo , M.P. Kalita , A.J. Boyland , A.S. Webb , R.J. Standish , J.K. Sahu , M.C. Paul , S. Das , S.K. Bhadra , M. Pal , Optics Communications **283,** (2010) 3423–3427.

[11] A. Halder, M.C. Paul, S.S.A. Damanhuri, N.A.D. Huri, A. Hamzah, S.W. Harun, H. Ahmad, S. Das, M. Pal and S.K. Bhadra "Upconversion luminescence in Tm3Y/Yb3Y co-doped double-clad silica fibers under 980 nm cladding pumping" Journal of Modern Optics **59**, (2012) 527–532.

[12] J. E. Townsend, S. B. Poole and D. N. Payne, Electron. Lett. **23**, (1987) 329-331.

[13] M.C.Paul, S.Bysakh, S.Das, S.K.Bhadra, M.Pal, S.Yoo, M.P. Kalita, A. J. Boyland, J.K.Sahu, Materials Science & Engineering B **175,** 108-119 (2010).

[14] M. C. Paul, S. Bysakh, S. Das, M.Pal, S. K. Bhadra, S. Yoo, A. J. Boyland and J. K. Sahu, The journal of Science of advanced materials, **4**, (2012) 1-29.

[15] M.C. Paul, M. Pal, A.V. Kir'yanov, S. Das, S.K. Bhadra, Yu.O. Barmenkov, A.A. Martinez-Gamez, and J.L. Lucio Martínez, Optics and Laser Technology **44,** (2012) 617–620.

[16] Arindam Halder, Mukul Chandra Paul, Sulaiman Wadi Harun, Shyamal Kumar Bhadra, Sandip Bysakh, Shyamal Das and Mrinmay Pal, Journal of Luminescence, **143**, (2013) 393–401.

[17] Bo Zhou, Hai Lin, and Edwin Yue-Bun Pun, Opt. Express **18**, (2010) 18805-18810.

[18] Pramod R. Watekar, Seongmin Ju, Seongjae Boo, Won-TaekHan, J. Non-Cryst. Solids **351**, (2005) 2446–2452.

[19] M. Inokuti, F. Hirayama, "Influence of energy transfer by the exchange mechanism on donor luminescence," J. Chem. Phys. **43**, (1965) 1978-1989.

[20] A. Braud, S. Girard, J. L. Doualan, M. Thuau, and R. Moncorge´, A. M. Tkachuk "Energy-transfer processes in Yb:Tm-doped KY3F10, LiYF4, and BaY2F8 single crystals for laser operation at 1.5 and 2.3 mm," Phys. Rev. B. **61**, (2000) 5280-5292.

[21] M. Laroche, S. G. Jayanta, K. Sahu, W. Clarkson, J. Nilsson **"**Accurate efficiency evaluation of energy-transfer processes in phosphosilicate Er3+–Yb3+-codoped fibers" J. Opt. Soc. Am. B **23**, (2006) 195-202.

[22] Dexter, D. "A theory of sensitized luminescence in solids" J. Chem. Phys. **21,** (1953) 836-850.

[23] P. Jander, W. S. Brocklesby, IEEE J. Quantum Electronics, **40,** (2004) 509-512.

[24] J. T. Kohli, S. R. A. Condrate, J. E. Shelby, Phys. Chem. Glasses, **34,** (1993) 81–87.

[25] J. K. Cristie, A. Tilocca, Chem. Mater. **22**, (2010) 3725-3734.

[26] D. A. Simpson, W. E. K. Gibbs, S. F. Collins, W. Blanc, B. Dussardier, G. Monnom, P. Peterka, G. W. Baxter, Opt. Express **16,** (2008) 13781-13799.

[27] YAG Yttrium Aluminium Garnet Laser Materials. VLOC Subsidiary of II-VI Incorporated, web: http://www.vloc.com